CHAPTER 14

NANOMATERIALS – THE NEXT GREAT CHALLENGE FOR QSAR MODELERS

TOMASZ PUZYN[1], AGNIESZKA GAJEWICZ[1], DANUTA LESZCZYNSKA[2], AND JERZY LESZCZYNSKI[3]

[1]*Laboratory of Environmental Chemometrics, Faculty of Chemistry, University of Gdańsk, ul. Sobieskiego 18/19, 80-952 Gdańsk, Poland, e-mail: puzi@qsar.eu.org*
[2]*Department of Civil and Environmental Engineering, Interdisciplinary Nanotoxicity Center, Jackson State University, Jackson MS 39217-0510, USA*
[3]*Department of Chemistry, Interdisciplinary Nanotoxicity Center, Jackson State University, Jackson MS 39217-0510, USA*

Abstract: In this final chapter a new perspective for the application of QSAR in the nanosciences is discussed. The role of nanomaterials is rapidly increasing in many aspects of everyday life. This is promoting a wide range of research needs related to both the design of new materials with required properties and performing a comprehensive risk assessment of the manufactured nanoparticles. The development of nanoscience also opens new areas for QSAR modelers. We have begun this contribution with a detailed discussion on the remarkable physical–chemical properties of nanomaterials and their specific toxicities. Both these factors should be considered as potential endpoints for further nano-QSAR studies. Then, we have highlighted the status and research needs in the area of molecular descriptors applicable to nanomaterials. Finally, we have put together currently available nano-QSAR models related to the physico-chemical endpoints of nanoparticles and their activity. Although we have observed many problems (i.e., a lack of experimental data, insufficient and inadequate descriptors), we do believe that application of QSAR methodology will significantly support nanoscience in the near future. Development of reliable nano-QSARs can be considered as the next challenging task for the QSAR community.

Keywords: Nanomaterials, Nanotoxicity, Nano-QSAR

14.1.   INCREASING ROLE OF NANOMATERIALS

The history of the "nanoworld" begun on December 29, 1959, being initiated by the classic talk given at the Annual Meeting of the American Physical Society by Richard P. Feyman [1]. "There's plenty of room at the bottom" – he summarized his visionary ideas about libraries as small as a pin head and miniature machines able to penetrate human body via the blood vessel and act as microscopic surgeons. The "nano" prefix, in a chemical context, describes particles characterized by at least

one diameter of 100 nm or less. When nanoparticles are intentionally synthesized to be used in consumer goods, they are called "nanomaterials" [2].

Nowadays, 50 years after Feyman's lecture, nanotechnology has emerged at the forefront of science and technology developments and nanomaterials have found a wide range of applications in different aspects of human life. For example, nanoparticles of such inorganic compounds as TiO_2 and ZnO oxides are used in cosmetics [3], sunscreens [3], solar-driven self-cleaning coatings [4], and textiles [5]. Nano-sized CuO has replaced noble metals in newer catalytic converters for the car industry [6]. Nanopowders of metals can be used as antibacterial substrates (e.g., the combination of the pure nanosilver ion with fiber to create antiodor socks) [7]. Finally, metal salts (i.e., CdSe quantum dots) have found many applications in electronics and biomedical imaging techniques [8, 9].

The discoveries of fullerene (C_{60}) in 1985 by Kroto et al. [10] and carbon nanotubes in 1991 by Iijima [11] opened a new area of the tailored design of carbon-based nanomaterials. Carbon-based nanomaterials are currently used, among other applications, for synthesis of polymers characterized by enhanced solubility and processability [12] and for manufacturing of biosensors [13]. They also contribute to a broad range of environmental technologies including sorbents, high-flux membranes, depth filters, antimicrobial agents, and renewable energy supplies [14].

According to current analysis [15], about 500 different products containing nanomaterials were officially on the market in 2007. Most of them (247) have been manufactured in the USA, 123 in East Asia (China, Taiwan, Korea, Japan), 76 in Europe, and only 27 in other countries. It is interesting that the number (500) is two times higher than the number of nanoproducts in the previous year. Investments in nanotechnology industry grew from $13 billion in 2004 to $50 billion in 2006 and – if one can believe the forecast – will reach $2.6 trillion in 2014.

Without doubt, nothing is able to stop such a rapidly developing branch of technology and we should be prepared for (better or worse) living day by day in symbiosis with nanomaterials.

14.2.   THEIR INCREDIBLE PHYSICAL AND CHEMICAL PROPERTIES

The astonishing physical and chemical properties of engineered nanoparticles are attributable to their small size. In the nanometer-scale, finite size effects such as surface area and size distribution can cause nanoparticles to have significantly different properties as compared to the bulk material [16]. For instance, by decreasing the size of gold samples one induces color changes from bright yellow through reddish–purple up to blue.

However, from the physico-chemical viewpoint, the novel properties of nanoparticles can also be determined by their chemical composition, surface structure, solubility, shape, ratio of particles in relation to agglomerates, and surface area to volume ratio. All these factors may give rise to unique electronic, magnetic, optical, and structural properties and, therefore, lead to opportunities for using nanomaterials in novel applications and devices [16].

New, characteristic properties of nanomaterials include greater hardness, rigidity, high thermal stability, higher yield strength, flexibility, ductility, and high refractive index. The band gap of nanometer-scale semiconductor structures decreases as the size of the nanostructure decreases, raising expectations for many possible optical and photonic applications [17].

With respect to the size of the grains, it has been suggested that nanomaterials would exhibit increased (typically 3–5 times) strength and hardness as compared to their microcrystalline counterparts. For example, the strength of nanocrystalline nickel is five orders of magnitude higher than that of the corresponding microcrystalline nickel [18]. Interestingly, the observed strength of crystalline nanomaterials is accompanied by a loss of ductility, which can result in a limitation of their utility [19]. However, some of the nanocrystalline materials have the ability to undergo considerable elongation and plastic deformation without failing (even up to 100–300%). Such machinability and superplasticity properties have been observed for ceramics (including monoliths and composites), metals (including aluminum, magnesium, iron, titanium), intermetallic elements (including iron, nickel, and titanium base), and laminates [20]. Although the atomic weight of carbon nanotubes is about one-sixth of the weight of steel, their Young's modulus and tensile strength are, respectively, five and 100 times higher than those of steel [21]. In addition, nanoparticles, because of their very small sizes and surface/interface effects such as the fundamental change in coordination, symmetry, and confinement, they may exhibit high magnetic susceptibility. A variety of nanoparticles reveal anomalous magnetic properties such as superparamagnetism. This opens new areas of potential application for them, such as data storage and ferrofluid technology [22].

According to recent studies, nanoparticles may have also great potential in medical application, mostly due to their good biocompatibility that allows them to promote electron transfer between electrodes and biological molecules. For instance, the high biocompatibility of magnetite nanocrystals (Fe_3O_4) makes them potentially useful as the magnetic resonance imaging contrast agents [23]. One of the unique aspects of nanoparticles is their high wettability, termed by Fujishima [24] as superhydrophilicity. Depending upon the chemical composition, the surface can exhibit superhydrophilic characteristics. For example, titanium dioxide (TiO_2), at sizes below a few nm, can decrease the water contact angle to $0\pm1°$ [24]. Nano-sized composites, due to the chemical composition and viscosity of the intercrystalline phase, may provide a significant increase in creep resistance. It has been demonstrated that alumina/silicon carbide composites are characterized by a minimum creep rate, three times lower than the corresponding monolith [25].

14.3. NANOMATERIALS CAN BE TOXIC

As mentioned in Section 14.1, different types of nanomaterials are increasingly being developed and used by industry. However, little is known about their toxicity, including possible mutagenic and/or carcinogenic effects [26]. Some recent contributions report evident toxicity and/or ecotoxicity of selected nanoparticles

and highlight the potential risk related to the development of nanoengineering. Evidently, there is insufficient knowledge regarding the harmful interactions of nanoparticles with biological systems as well as with the environment.

14.3.1.   Specific Properties Cause Specific Toxicity

It is well known that the most important parameters with respect to the induction of adverse effects by a xenobiotic compound are its dose, dimension, and durability. Conversely, it is well established that nano-sized particles, due to their unique physical and chemical properties discussed above, behave differently from their larger counterparts of the same chemical composition [26–31]. Because of the difference between nanoparticles and bulk chemicals, the risk characterization of bulk materials cannot be directly extrapolated to nanomaterials.

The biological activity of nanoparticles and their unique properties causing harmful effects are highly dependent on their size. Nanoparticles, because of their small size, may pass organ barriers such as skin, olfactory mucosa, and the blood–brain barrier [32–34], readily travel within the circulatory system of a host, and deposit in target organs. This is not possible with the same material in a larger form [35]. Indeed, reduction of the particle's size to the nanoscale level results in a steady increase of the surface to volume ratio. As a consequence, a larger number of potentially active groups per mass unit is "available" on the surface and might interact with biological systems [35]. This is one possible explanation why nano-sized particles of a given compound are generally more toxic than the same compound in its larger form [36].

However, Oberdörster et al. [37] suggested that the particle size is not the only possible factor influencing toxicity of nanomaterials. The following features should be also considered:

- size distribution,
- agglomeration state,
- shape,
- porosity,
- surface area,
- chemical composition,
- structure-dependent electronic configuration,
- surface chemistry,
- surface charge, and
- crystal structure.

Natural and anthropogenic nanoparticles gain access into the human body through the main ports of entry including the lungs, the skin, or the gastrointestinal tract. The unique properties of nanoparticles allow them not only to pnetrate physiological barriers but also to travel throughout the body and interact with subcellular structures. Toxicological studies show that nanoparticles can be found in various cells such as mitochondria [38, 39], lipid vesicles [40], fibroblasts [41], nuclei [42], and macrophages [43].

14.3.2. Oxidative Stress

Depending on their localization inside the cell, nanoparticles can induce formation of reactive oxygen species (ROS), for instance, superoxide radicals, hydroxyl radicals reactive nitrogen [44], sulfur [45], and other species stressing the body in a similar manner to the effect of ROS [46]. This results in oxidative stress and inflammation, leading to the impacts on lung and cardiovascular health [16].

It is worth noting that normally, due to the presence of antioxidant molecules (i.e., vitamin C and glutathione), the body's cells are able to defend themselves against ROS and free radicals damage. However, when a large dose of strongly electrophilic nanoparticles enter the body, the balance between reduced glutathione (GSH) and its oxidized form (GSSG) is destroyed [47] and the unscavenged oxidants cause cell injuries by attacking DNA, proteins, and membranes [48]. At the cellular level, oxidative stress is currently the best developed paradigm depicting the harmful effects of nano-sized particles [31, 49, 50].

14.3.3. Cytotoxicity and Genotoxicity

The mechanism of oxidative stress occurring at the molecular level is mainly responsible for observed cytotoxic and genotoxic effects induced by nanoparticles. Cytotoxicity of selected nanospecies has been confirmed by many researchers. For example, fullerene (C_{60}) particles suspended in water are characterized by antibacterial activity against *Escherichia coli* and *Bacillus subtilis* [51] and by cytotoxicity to human cell lines [52]. Single multiwalled carbon nanotubes (CWCNTs and MWCNTs) are also toxic to human cells [41, 53]. Nano-sized silicon oxide (SiO_2), anatase (TiO_2), and zinc oxide (ZnO) can induce pulmonary inflammation in rodents and humans [54–56].

Epidemiological studies have shown that nanoparticles might be genotoxic to humans [57]. Irreversible DNA modifications resulting from the activity of ROS may lead to heritable mutations, involving a single gene, a block of genes, or even whole chromosomes. DNA damage may also disrupt various normal intracellular processes, such as DNA replication and modulate gene transcription, causing abnormal function or cell death [16, 44, 58]. Until now, more than 100 different oxidative DNA lesions have been found. The most investigated OH-related DNA lesions is 8-hydroxydeoxyguanosine (8-OHdG) [59], which may be induced by several particles such as asbestos, crystalline silica, coal fly ashes. Oxygen free radicals may overwhelm the antioxidant defense system by mediating formation of base adducts, such as 8-hydroxydeoxyguanosine, and therefore play a key role in initiation of carcinogenesis [60].

14.3.4. Neurotoxicity

Data on neurotoxic effects of engineered nanoparticles are very limited, but it has been reported that inhaled nanoparticles, depending on their size, may be distributed to organs and surrounding tissues, including the olfactory mucosa or bronchial

epithelium and then can be translocated via the olfactory nerves to the central nervous system [61]. There is also some evidence that nano-sized particles can penetrate and pass along nerve axons and dendrites of neurons into the brain [33]. Recent studies confirm the translocation of nanoparticles from the respiratory tract into the central nervous system; for example, inhalation with 30 nm magnesium oxide in rats showed that manganese can be taken up into olfactory neurons and accumulated in the olfactory bulb [34].

The particles at the nanoscale may also gain access to the brain across the blood–brain barrier [2]. There is experimental evidence that oxidative stress also plays an important role in neurodegenerative diseases and brain pathology, for instance, Hallervorden-Spatz Syndrome, Pick's disease, Alzheimer's disease, or Parkinson's disease [62].

14.3.5.   Immunotoxicity

The effects of nanoparticles on the immune system are still unclear. Although the reticuloendothelial system (RES) is able to eliminate nanoparticles, several toxicological studies have suggested that nanoscale particles' interaction with the defense activities of immune cells can change their antigenicity and stimulate and/or suppress immune responses. Direct experiments showed that dendritic cells and macrophages uptake of nanoparticle–protein complexes may change the formation of the antigen and initiate an autoimmune response [16]. Several studies have also reported that nanoparticles may induce damage to red blood cells (erythrocytes). Bosi et al. [63] have studied the hemolytic effect of different water-soluble C_{60} fullerenes. Preliminary results indicate that hemolytic activity depends on the number and position of the cationic surface groups. However, no clinically relevant toxicity has yet been demonstrated [64].

14.3.6.   Ecotoxicity

Nano-sized particles such as volcanic ash, dust storms, or smoke from natural fires have always been present in the environment. However, the recent progress of industry has increased engineered nanoparticle pollution. The unique size-specific behavior and specific physical–chemical properties, in combination with toxicity to particular living organisms, may also result in harmful effects on the level of whole environmental ecosystems [65].

In the pioneering report on the non-human toxicity of fullerene, Eva Oberdörster [66] observed that manufactured nanomaterials can have negative impacts on aquatic organisms. Water-soluble C_{60} fullerenes cause oxidative damage (lipid peroxydation in the brain) and depletion of glutathione in the gill of juvenile largemouth bass (*Micropterus salmoides*) at a concentration of 0.5 ppm. However, these results might be disputable, because the authors used the organic solvent tetrahydrofuran (THF) to disaggregate C_{60} fullerenes, THF is classified as a neurotoxin [67].

Subsequently, Lover and Klaper [68] observed the toxicological impact of nanoparticles of fullerenes (C_{60}) and titanium dioxide (TiO_2) to *Daphnia magna*: C_{60} and TiO_2 caused mortality with a LC_{50} value of 5.5 ppm for TiO_2 and a

LC_{50} value of 460 ppb for the fullerene. In this case the authors also used THF for solubilization of hydrophobic C_{60}, thus the results are also of lower credibility. Interestingly, in similar experiments by Andrievsky et al. [69] with "fullerene water solutions" (hydrated fullerenes, $C_{60} \cdot nH_2O$), no mortality was observed.

In a later study, Adams et al. [70] confirmed the acute toxicity of selected nano-sized metal oxides against *D. magna*. He observed that SiO_2 particles were the least toxic and that toxicity increased from SiO_2 to TiO_2 to ZnO. A further study by the authors [71] showed that these three photosensitive nanoscale metal oxides in water suspensions have similar antibacterial activity to Gram-positive (*B. subtilis*) and Gram-negative (*E. coli*) bacteria ($SiO_2 < TiO_2 <$ ZnO). All the metal oxides nanoparticles tested inhibited the growth of both Gram-positive and Gram-negative bacteria; however, *B. subtilis* was more sensitive than *E. coli*.

Similar results have been observed for a bath of ZnO, TiO_2, and CuO against bacterium *Vibrio fischeri* and crustaceans *D. magna* and *Thamnocephalus platyurus* [72]. The antibacterial effects of nano-sized metal oxides to *V. fischeri* were similar to the rank of toxicity to *D. magna* and *T. platyurus*; they increased from TiO_2 to CuO and ZnO. It is also very important to recognize that titanium dioxide was not toxic even at the 20 g/l level, which means that not all nanoparticles of metal oxides induce toxicity.

Smith et al. [73] investigated the ecotoxicological potential of single-walled carbon nanotubes (SWCNT) to rainbow trout (*Oncorhynchus mykiss*) showing that the exposure to dispersed SWCNT causes respiratory toxicity – an increase of the ventilation rate, gill pathologies, and mucus secretion. Additionally, the authors observed histological changes in the liver, brain pathology, and cellular pathologies, such as individual necrotic or apoptotic bodies, in rainbow trout exposed to 0.5 mg/l SWCNT.

Mouchet et al. [74] analyzed the acute toxicity and genotoxicity of double-walled carbon nanotubes (DWNTs) to amphibian larvae (*Xenopus laevis*). The authors did not observe any effects at concentrations between 10 and 500 mg/l. However, at the highest concentrations (500 mg/l) 85% of mortality was measured, while at the lowest concentrations (10 mg/l) reduced size and/or a cessation of growth of the larvae were observed.

Summarizing this section, there is strong evidence that chemicals, when synthesized at the nanoscale, can induce a wide range of specific toxic and ecotoxic effects. Moreover, even similar compounds from the same class can differ in toxicity. The available data on toxicity are still lacking; thus, more comprehensive and systematic studies in this area are necessary and very important.

14.4. "NANO-QSAR" – ADVANCES AND CHALLENGES

As demonstrated in this book, quantitative structure–activity relationship (QSAR) methods can play an important role in both designing new products and predicting their risk to human health and the environment. However, taking into account the specific properties of nanomaterials and their still unknown modes of toxic action, this class of compounds seems to be much more problematic for QSAR modelers than the "classic" (small, drug-like) chemicals.

14.4.1.   Description of Structure

Until now, more than 5000 different descriptors have been developed and used for the characterization of molecular structure (Chapter 3). In general, the descriptors can be classified according to their dimensionality. Constitutional descriptors, so-called "zero-dimensional," are derived directly from the formula (e.g., the number of oxygen atoms). Descriptors of bulk properties, such as n-octanol/water partition coefficient or water solubility, are classified as "one-dimensional" descriptors. Topological descriptors based on the molecular graph theory are called "two-dimensional" descriptors and characterize connections between individual atoms in the molecule. "Three-dimensional" descriptors reflect properties derived from the three-dimensional structure of a molecule optimized at the appropriate level of quantum-mechanical theory. "Four-dimensional" descriptors are defined by molecular properties arising from interactions of the molecule with probes characterizing the surrounding space or by stereodynamic representation of a molecule, including flexibility of bonds, conformational behavior, etc. [75–79]. Only a little is known about applicability of those "traditional" descriptors for the characterization of nanostructures. Some authors [80–82] postulate that the existing descriptors are insufficient to express the specific physical and chemical properties of nanoparticles. Thus, novel and more appropriate types of the descriptors must be developed.

A group of nanoparticles is structurally diversified. In fact, this group has been defined arbitrarily in some way, taking into account size as the only criterion of the particles' membership. Therefore, structures as various as nanotubes, fullerenes, crystals, and atom clusters as well as chemical species of such different properties as metals, non-metals, organic compounds, inorganic compounds, conductors, semi-conductors, and isolators were put together into one single group. Since nanoparticles are not structurally homogenous, a common mechanism of toxicity cannot be expected for all of them. In consequence, toxicity and other properties should be studied within the most appropriately chosen sub-classes of structural and physico-chemical similarity.

What is the best way to define the sub-classes? The answer might be given based on a stepwise procedure recommended by the OECD guidance document on the grouping of chemicals [83] (see also Chapter 7). Along with the guidelines, the following eight steps should be performed:

1. Development of the category hypothesis, definition, and identification of the category members. The category can be defined based on chemical similarity, physico-chemical properties, toxicological endpoint, and/or mechanism of action, as well as in terms of a metabolic pathway.
2. Gathering of data for each category members. All existing data should be collected for each member of the category.
3. Evaluation of available data for adequacy. The data should be carefully evaluated at this stage according to the commonly accepted protocols (i.e., according to the appropriate OECD guidance).
4. Construction of a matrix of data availability (category endpoints vs. members). The matrix is to indicate whether data are available or not.

5. Performing of a preliminary evaluation of the category and filling data gaps. The preliminary evaluation should indicate if (i) the category rationale is supported and (ii) the category is sufficiently robust for the assessment purpose (contains sufficient, relevant and reliable information).
6. Performing of additional testing (experiments). Based on the preliminary evaluation (especially evaluation of the robustness), additional experiments and group members for testing can be proposed.
7. Performing of a further assessment of the category. If new data from the additional testing are generated, the category should be revised according to the criteria from step 5.
8. Documenting of the finalized category. Finally, the category should be documented in the form of a suitable reporting format proposed by the guidance.

The currently proposed [82] working classification scheme for nanostructured particles includes nine categories:

1. spherical or compact particles;
2. high aspect ratio particles;
3. complex non-spherical particles;
4. compositionally heterogeneous particles – core surface variation;
5. compositionally heterogeneous particles – distributed variation;
6. homogeneous agglomerates;
7. heterogeneous agglomerates;
8. active particles;
9. multifunctional particles.

This classification has been adapted from the original work of Maynard and Aitken [84].

What types of structural properties should be described within the groups? As previously discussed in Section 14.3, the diameter of a nanoparticle is important, but it is not the only one possible factor influencing the mode of toxic action. The additional structural characteristics which must also be appropriately expressed are size distribution, agglomeration, shape, porosity, surface area, chemical composition, electronic configuration, surface chemistry, surface charge, and crystal structure. In contrast to the classic QSAR scheme, an entire characterization of a nanostructure may be impossible only when computational methods are employed. Novel descriptors reflecting not only molecular structure, but also supra-molecular pattern (size, shape of the nanoparticles, etc.) should be derived from both computational and experimental techniques.

The fastest and relatively easy step of characterizing the structure is the calculation of constitutional and topological descriptors. An interesting and very practical idea in this field is to replace a series of simple descriptors by one, so-called "technological attributes code" or "SMILES-like code" [85–88]. For instance, a nanoparticle of ceramic zirconium oxide, existing in bulk form and synthesized at a temperature of 800°C can be expressed by the code "Zr,O,O,CER,%E" [80]. Similar to the simplified molecular input line entry system (SMILES), the international

chemical identifier (InChI) might also be used directly as a descriptor of chemical composition [89]. Another possibility is to apply descriptors derived from either molecular graph (MG) or the graphs of atomic orbitals (GAO) theory [90–92]. In the first case, vertexes in the graph represent atoms, while edges represent covalent bonds. In the second method, vertexes refer to particular atomic orbitals (1s, 2s, 2p, etc.), while edges connect the orbitals belonging to different atoms (Figure 14-1). Based on the molecular graphs, Faulon and coworkers [93–96] have developed the signature molecular descriptor approach for the characterization of fullerenes and nanotubes. The signature is a vector including extended valences of atoms derived from a set of subgraphs, following the five-step algorithm:

1. constructing of a subgraph containing all atoms and bonds that are at a distance no greater than the given signature height;
2. labeling the vertices in a canonical order;
3. constructing a tree spanning all the edges;
4. removing of all canonical labels that appear only one time;
5. writing the signature by reading the tree in a depth-first order.

The signature descriptor can be utilized not only for direct QSAR modeling, but also for calculating a range of topological indices (i.e., the Wiener index).
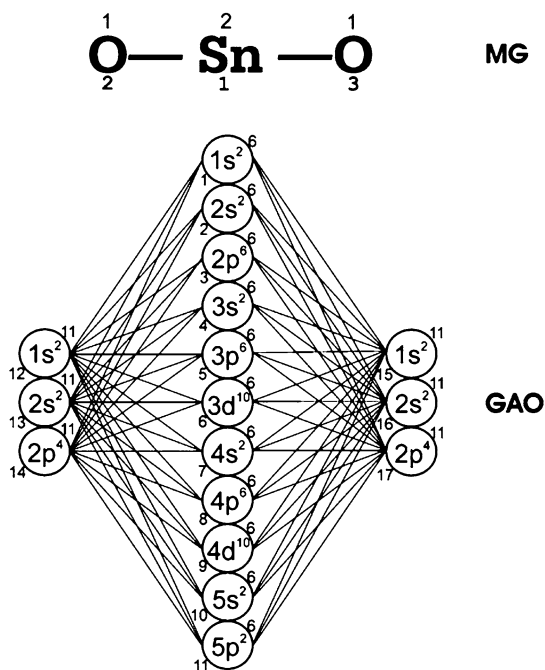

Figure 14-1. Molecular graph (MG) and graph of atomic orbitals (GAO) for SnO_2 (vertex numbering and vertex degrees). [90–92, 132]

Without doubt, simplicity of calculation is the most significant advantage of the topological descriptors. However, in many cases these two-dimensional characteristics are insufficient to investigate more complex phenomena. In such a situation, a more sophisticated approach must be employed to describe the structure appropriately. As mentioned previously, quantum-mechanical calculations can deliver useful information on the three-dimensional features (see Chapter 2). Among others, they include: molecular geometry (bond lengths, valence, and torsion angles), electron distribution, ionization potential, electron affinity, surface reactivity, and band gap. When performing quantum-mechanical calculations, there are always two important assumptions to be introduced. First one is an appropriate molecular model; the second one is the appropriate level of the theory. Both assumptions are closely related: when the model (system) is too large, the calculations at the highest levels of the theory are impossible, because of large computational time and other technical resources to be required [97].

Small fullerenes and carbon nanotubes can be treated as whole systems and modelled directly with quantum-mechanical methods. Among the theory levels, the density functional theory (DFT) recently seems to have been accepted as the most appropriate and practical choice for such calculations. Indeed, DFT methods can serve as a good alternative for conventional ab initio calculations, when a step beyond the means field approximation is crucial and the information on the electron correlation significantly improves the results (e.g., Hartree–Fock – HF method in conjunction with Møller-Pleset the second-order correction – MP2). Unfortunately, even "small" fullerenes and carbon nanotubes (containing between 40 and 70 carbon atoms) are, in fact, large from quantum-mechanical point of view. Therefore, the "classic" ab initio calculations might be impractical because of the reasons mentioned in the previous paragraph, whereas DFT can be performed in reasonable time.

The functional commonly utilized for DFT is abbreviated with the B3LYP symbol. In B3LYP calculations (Eq. 14-1) the exchange-correlation energy E_{XC} is expressed as a combination (a_0, a_X, and a_C are the parameters) of four elements: (i) the exchange-correlation energy from the local spin density approximation (LSDA, E_{xc}^{LSDA}), (ii) the difference between the exchange energy from Hartree–Fock (E_X^{HF}) and LSDA (E_X^{LSDA}), (iii) Becke's exchange energy with gradient correction (E_X^{B88}), and (iv) the correlation energy with Lee-Yang-Parr correction (E_c^{LYP}) [98, 99]:

$$E_{XC} = E_{XC}^{LSDA} + a_0(E_X^{HF} - E_X^{LSDA}) + a_X E_X^{B88} + a_C E_C^{LYP} \qquad (14\text{-}1)$$

Sometimes, when a system is too large from the quantum-mechanical point of view, the calculations are practically impossible. The situation is very common for larger crystalline nanoparticles (i.e., nanoparticles of metal oxides: TiO_2, Al_2O_3, SnO_2, ZnO, etc.) and, in such cases, a simplified model of the whole structure must first be appropriately selected. In general, there are two strategies for modeling of crystalline solids: (i) an application of the periodic boundary conditions (PBSs) and (ii) calculations based on the molecular clusters. In the first approach, calculations for a single unit cell are expanded in the three dimensions with respect to the

translational symmetry by employing appropriate boundary conditions (i.e., the unit cell should be neutral and should have no dipole moment). In doing so, the model includes information on the long-range forces occurring in the crystal. However, the cell size should be large enough to also be able to model defects in the surface and to eliminate the spurious interactions between periodically repeated fragments of the lattice [100–102].

In the second approach, a small fragment or so-called "cluster," is cut off from the crystal structure and then used as a simplified model for calculations. The only problem is how to choose the diameter of the cluster correctly? This must be performed by reaching a compromise between the number of atoms (and thus the required time of computations) and the expected accuracy (and hence level of the theory to be employed). It is worth mentioning that the molecular properties can be divided into two groups depending on how they change with increasing size of the cluster (going from molecular clusters to the bulk form). They are (i) scalable properties, varying smoothly until reaching the bulk limit and (ii) non-scalable properties, when the variation related to increasing size of the cluster is not monotonic. Although the cluster models usually avoid the long-range forces, they have found many applications in modeling of local phenomena and interactions on the crystal surface [103].

As previously mentioned, in addition to calculated properties, experimentally derived properties may also serve as descriptors for developing nano-QSARs (Table 14-1). The experimental descriptors seem to be especially useful for expressing size distribution, agglomeration state, shape, porosity, and irregularity of the surface area. Interestingly, the experimental results can be combined with numerical methods to define new descriptors. For example, images taken by scanning electron microscopy (SEM), transmission electron microscopy (TEM), or atomic force

Table 14-1. Experimental properties for possible use as descriptors in nano-QSAR studies [105]

Properties	Instruments and methods*
Diameter	EM, AFM, Flow-FFF, DLS
Volume	Sed-FFF
Area	EM, AFM
Surface charge	z-Potential, electrophoretic mobility
Crystal structure	XRD, TEM-XRD
Elemental composition	Bulk: ICP-MS, ICP-OES Singe nanoparticle: TEM-EDX Particle population: FFF-ICP-MS
Aggregation state	DLS, AFM, ESEM
Hydrophobicity	Liquid–liquid extraction chromatography
Hydrodynamic diameter	Flow-FFF, DLS
Equivalent pore size diameter	Particle filtration

*Abbreviations: EM – electronic microscopy, AFM – atomic force microscopy, FFF – field flow filtration, DLS – dynamic light scattering, LC – liquid chromatography, XRD – X-ray diffraction, TEM – transmission electron microscopy, ICP-MS – inductively coupled plasma mass spectrometry, ICP-OES – inductively coupled plasma emission spectroscopy, EDX – energy dispersive X-ray spectrometry, ESEM – environmental scanning electron microscopy.
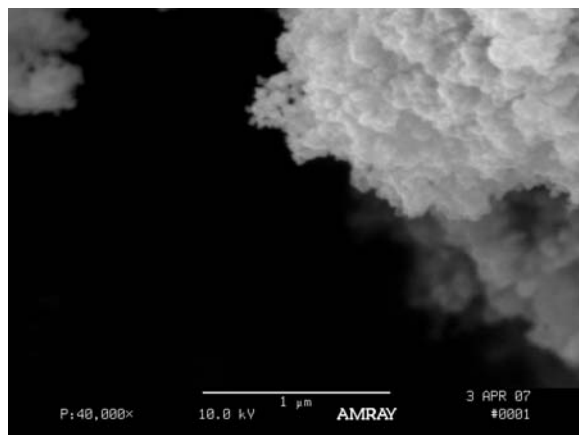
Figure 14-2. Nanopowder – SEM image of nano-sized SnO_2

microscopy (AFM) (Figure 14-2) might be processed with use of novel chemometric techniques of image analysis. Namely, a series of images for different particles of a given nanostructure should first be taken. Then, the pictures must be numerically averaged and converted into a matrix containing numerical values that correspond to intensity of each pixel in the gray scale or color value in the RGB scale. New descriptors can be defined based on the matrix (i.e., a shape descriptor can be calculated as a sum of non-zero elements in the matrix; porosity – as a sum of relative differences between each pixel and its "neighbors," etc.) [104].

Without doubt, an appropriate characterization of the nanoparticles' structure is currently one of the most challenging tasks in nano-QSAR. Although more than 5000 QSAR descriptors have been defined so far, they may be inadequate to express the supramolecular phenomena governing the unusual activity and properties of nanomaterials. As a result, much more effort in this area is required.

14.4.2. Nanostructure – Electronic Properties Relationships

An important step related to the numerical description of chemical structure and QSAR modeling involves establishing a qualitative relationship between the structure of a nanoparticle and its various electronic properties.

The B3LYP functional and the standard 6-31G(d) Polple's style basis set were applied by Shukla and Leszczynski [106] to investigate the relationships between the shape, size, and electronic properties of small carbon fullerenes, nanodisks, nanocapsules, and nanobowls. They found out that the ionization potentials decrease, while the electron affinities increase in going from the C_{60} fullerenes to the closed nanodisks, capsules, and open bowl-shaped nanocarbon clusters. In similar studies performed for capped and uncapped carbon nanotubes at the B3LYP/6-31G(d) level of theory by Yumura et al. [107, 108], the authors demonstrated that the tube lengths, edge structures, and end caps play an important role in determining the

band gap expressed as a difference between the energies of the highest occupied and lowest unoccupied molecular orbitals (HOMO–LUMO) and vibrational frequencies. Wang and Mezey [109] characterized electronic structures of open-ended and capped carbon nanoneedles (CNNs) at the same theory level (B3LYP/6-311G(d)) concluding that conductivity of the studied species is strictly correlated to their size. Only very long CNNs structures have band gaps sufficiently narrow to be semiconductors, while the band gaps of very short and thin structures are too large to conduct electrons. Similarly, Poater et al. [110, 111] observed that the Parr electrophilicity and electronic movement described by the chemical potential increase with increasing length of the carbon nanoneedles and very "short" structures (containing four layers and less) have a HOMO–LUMO gap too large to allow conductivity. Moreover, Simeon et al. [112], by performing B3LYP calculations, demonstrated that a replacement of the fullerene carbon atom with a heteroatom results in a significant change of electronic and catalytic properties of the fullerene molecule.

Similar studies have been performed for crystalline metal semi-conductors with the use of the cluster calculations. As mentioned in Section 14.4.1, some electronic properties are scalable. They change with the changing size of the cluster until the bulk limit is reached. Known examples of such properties are the HOMO–LUMO gap (band gap) and the adiabatic electron detachment energy. For instance, the band gap of ZnO nanoparticles decreases with increasing diameter of the particle up to the bulk value observed for about 4 nm [113]. Similarly, the bulk limits of the HOMO–LUMO gap and the detachment energy for titanium oxide anion clusters of increasing size (increasing n) were reached already for n=7 [114, 115].

In the classic formalization of QSARs, electronic properties (e.g., HOMO, LUMO, ionization potential) have been utilized as "ordinary" molecular descriptors. As discussed above, this approach should be revised for nanoparticles, for which the properties vary with size of a particle and this variation cannot be simply described by a linear function. It is not out of the question that similar phenomena might be observed also for other types of the "traditional" descriptors and further studies in this area are required and strongly justified.

14.4.3.   Nano-QSAR Models

Regarding the five OECD principles for the validation of a (Q)SAR as discussed in Chapters 12 and 13, an ideal QSAR model, applicable for regulatory purpose, should be associated with (i) a well-defined endpoint; (ii) an unambiguous algorithm; (iii) a defined domain of applicability; (iv) appropriate measures of goodness-of-fit, robustness, and predictivity; and (v) a mechanistic interpretation, if possible. Unfortunately, it is extremely difficult to fulfill all of these principles for (Q)SARs applicable to nanomaterials. There are two main difficulties related to the development of nano-QSARs. The first one is lack of sufficiently numerous and systematic experimental data, while the second one is very limited knowledge on mechanisms of toxic action.

As we mentioned many times, regarding their structure, the class of nanomaterials is not homogenous, combining a range of physico-chemical properties, as

well as possible mechanisms of metabolism and toxicity. Thus, it is impossible to assume one common applicability domain for all nanomaterials. Each mode of toxicity and each class of nanomaterials should be studied separately. Analyzing the literature data (Section 14.3) it must be concluded that even if a class of structurally similar nanoparticles is tested with the same laboratory protocol, the number of tested compounds is often insufficient to perform comprehensive internal and external validation of a model and to calculate the appropriate measures of robustness and predictivity in QSAR. For instance, Limbach et al. [116] have proposed two rankings of cytotoxicity of seven oxide nanoparticles based on the in vitro study of human and rodent cells. The rankings were as follows: (i) $Fe_2O_3 \approx$asbestos > ZnO > $CeO_2 \approx ZrO_2 \approx TiO_2 \approx Ca_3(PO_4)_2$ and (ii) ZnO > asbestos$\approx ZrO_2$ > $Ca_3(PO_4)_2 \approx Fe_2O_3 \approx CeO_2 \approx TiO_2$, respectively, for human (mesothelinoma) and rodent cells. In another paper by the same research group, the authors have found that for four metal nanoparticles – namely, TiO_2, Fe_2O_3, Mn_3O_4, and Co_3O_4 – the chemical composition was the main factor determining the formation of reactive oxygen responsible for toxicity toward human lung epithelial cells [117]. Obviously, the results cannot be combined together and a data set containing five or six compounds is too small to build an appropriately validated QSAR model.

Do these restrictions and problems mean QSAR modelers are not able to provide useful and reliable information for nanoparticles? We do not believe this to be true. The amount of data will increase along with increasing number of nanotoxicological studies. However, no one can expect the accumulation in the next few years of such extensive data for nanomaterials, as it is now available for some environmental pollutants, pharmaceuticals, and "classical" industrial chemicals [118, 119]. Despite the limitations, there are some very promising results of preliminary nano-QSAR studies which are reviewed below.

Toropov et al. [81] have developed two models defining the relationships between basic physico-chemical properties (namely, water solubility, log S, and n-octanol/water partition coefficient, log P) of carbon nanotubes and their chiral vectors (as structural descriptors). The two-element chiral vector (n, m) contains information about the process of rolling up the graphite layer when a nanotube is formed. It had been previously known [120] that the elements of the chiral vector are related to conductivity. At this point, Toropov et al. confirmed, using the QSPR-based research, that the vector is also strictly related to other properties. The models developed were defined by the following two equations (Eqs. 14-2 and 14-3):

$$\log S = -5.10 - 3.51n - 3.59m$$
$$R^2 = 0.99,\ s = 0.053,\ F = 126$$

$$\text{(14-2)}$$

$$\log P = -3.92 + 3.77n - 3.60m$$
$$R^2 = 0.99,\ s = 0.37,\ F = 2.93$$

$$\text{(14-3)}$$

The study was based on experimental data being available for only 16 types of carbon nanotube. To perform an external validation, the authors divided the

compounds into a training set ($n=8$) and a test set ($n_{\text{test}}=8$). Statistics of the validation were $R^2_{\text{test}} = 0.99$, $s_{\text{test}}=0.093$, and $F_{\text{test}}=67.5$ and $R^2_{\text{test}}=0.99$, $s_{\text{test}}=0.29$, and $F_{\text{test}}=5.93$, respectively, for the models for water solubility and n-octanol/water partition coefficient. Without doubt, these were the first such QSPR models developed for nanoparticles. However, the ratio of descriptors to compounds (the Topliss ratio) was low, thus the model might be unstable (see discussion in Chapter 12 for more detail).

Another contribution by Toropov and Leszczynski [80] presents a model predicting Young's modulus (*YM*) for a set of inorganic nanostructures (Eq. 14-4).

$$YM = -3720.0(\pm 39.9) + 3950.0(\pm 39.2)DCW$$
$$R^2 = 0.98, \, s = 18.3, \, F = 761,$$
$$R^2_{\text{test}} = 0.90, \, s_{\text{test}} = 34.7, \, F_{\text{test}} = 51$$
$$(14\text{-}4)$$

The model was calibrated with a training set of 21 compounds and validated with eight compounds, thus the Topliss ratio in this case was satisfactory. The values of *DCW* descriptor were calculated from the Smiles-like code, according to the following equation (Eq. 14-5):

$$DCW = \prod_{k=1}^{N} CW(I_k) \qquad (14\text{-}5)$$

where I_k is the component information on the nanostructure (e.g., Al, N, BULK, refer to Section 14.4.1), $CW(I_k)$ is the correlation weight of the component I_k, and N is the total number of these components in a given nanostructure. The values of $CW(I_k)$ were calculated by the Monte Carlo method with the software developed by the authors. The model was correctly validated and the authors demonstrated the possibility of the prediction the Young's modulus for external compounds with QSAR.

Martin et al. [121] have proposed two QSAR models predicting the solubility of buckminsterfullerene (C_{60}), respectively, in n-heptane (log S_{heptane}) and n-octanol (log S_{octanol}) (Eqs. 14-6 and 14-7):

$$\log S_{\text{heptane}} = 3.49(\pm 3.46) + 76.98(\pm 8.11)RNCG - 9.56(\pm 2.25)^2ASIC$$
$$-1.18(\pm 0.45)E_{\text{ee}}^{\min}(CC)$$
$$n = 15, \, R^2 = 0.90, \, s^2 = 0.18, \, F = 34.8,$$
$$n_{\text{test}} = 3, \, Q^2 = 0.84, \, R^2_{50} = 0.82, \, s^2_{50} = 0.35$$
$$(14\text{-}6)$$

$$\log S_{\text{octanol}} = 10.5(\pm 1.30) - 8.40 \times 10^{-2}(\pm 7.71 \times 10^{-3})^1IC - 1.57(\pm 0.16)$$
$$E_{\text{ee}}^{\min}(CC) + 0.88(\pm 0.15)RPCS$$
$$R^2 = 0.96, \, s^2 = 0.078, \, F = 97.3,$$
$$Q^2 = 0.93, \, R^2_{50} = 0.96, \, s^2_{50} = 0.10$$
$$(14\text{-}7)$$

The symbols R_{50}^2 and s_{50}^2 refer to leave-50%-out cross-validation. The authors applied CODESSA descriptors, namely, *RNCG* – relative negative charge (Zefirov's PC); ^2ASIC – average structural information content of the second order; E_{ee}^{min} (CC) – minimum exchange energy for a C–C bond; ^1IC – first-order information content; and *RPCS* – relative positive charged surface area. Interestingly, the models were calibrated on 15 compounds including 14 polycyclic aromatic hydrocarbons (PAHs) containing between two and six aromatic rings and the fullerene. Although values of solubility predicted for the fullerene seem to be reasonable, the authors did not validate the applicability domain of the models. Indeed, the structural difference between 14 hydrocarbons and the fullerene is probably too large to make reliable predictions for C_{60} (the polycyclic hydrocarbons are planar, but the fullerene is spherical). In addition, the experimental values of log *S* for 14 PAHs ranged from -3.80 to 0.22 in heptane and from -3.03 to -0.02 in octanol, while the experimental values for the fullerene were -4.09 and 4.18 in heptane and octanol, respectively.

An interesting area of nano-QSAR applications is estimating solubility of a given nanoparticle in a set of various solvents. In that case, the main purpose of molecular descriptors is to correctly characterize the variation in interactions between the particle and the molecules of different solvents [122]. In fact, it means that the descriptors are related to the structure of solvents rather than to the nanoparticle structure.

Murray et al. [123] have developed a model characterizing the solubility of C_{60} in 22 organic solvents by employing three following descriptors: two quantities, σ_{tot}^2 and υ reflecting variability and degree of balance of electrostatic potential on the solvent surface and the surface area, *SA* (Eq. 14-8).

$$\log(S \times 10^4) = -29.0 \left[\sigma_{tot}^2/(SA)^{3/2}\right] + 1.28 \left(\upsilon\sigma_{tot}^2\right)^{1/2} + 1.53 \times 10^{-9}(SA)^4 - 2.72$$
(14-8)

Although the model is well fitted ($R=0.95$, $s=0.48$), nothing is known about its predictive ability, because the model has not been validated.

A set of linear models built separately for individual structural domains, namely alkanes ($n=6$), alkyl halides ($n=32$), alcohols ($n=6$), cycloalkanes ($n=6$), alkylbenzenes ($n=16$), and aryl halides ($n=9$), was published by Sivaraman et al. [124]. The models were based on connectivity indices, numbers of atoms, polarizability, and variables indicating the substitution pattern as molecular descriptors for the solvents. The values of R^2 for particular models ranged between 0.93 (alkyl halides) and 0.99 (cycloalkanes) with the corresponding values of *s* from 0.22 (alkyl halides) to 0.04 (cycloalkanes). The authors concluded that it was impossible to obtain a unified model that included all solvents. However, when the first three classes of solvents (i.e., alkanes, alkyl halides, and alcohols) were combined together into one model, the results of an external validation performed were satisfactory.

As well as linear approaches, non-linear models have been constructed. For instance, Kiss et al. [125] applied an artificial neural network utilizing molar volume, polarizability parameter, LUMO, saturated surface, and average polarizability as structural descriptors of solvents. They observed that for most of the solvents

studied ($n=126$) solubility decreases with increasing molar volume and increases with polarizability and the saturated surface areas of the solvents. The reported value of s in that case was 0.45 of log units. The values of R^2 and F were 0.84 and 633, respectively.

In another study [126] the authors proposed modeling with both multiple linear regression with heuristic selection of variables (HM-MLR) and a least-squares support vector machine (SVM). Then they compared both models with each other. Both models were developed with CODESSA descriptors [127]. Interestingly, the results were very similar (the model using SVM had slightly better characteristics). The values of R^2 for the linear and non-linear model were, respectively, 0.89 and 0.90, while the values of F were 968 and 1095. The reported root mean square errors were 0.126 for the linear model (HM-MLR) and 0.116 for the model employing SVM. When analyzing all the results it might be concluded that the main factor responsible for differences in the model error is related to the type of the descriptors rather than to the mathematical method of modeling.

Recently, Toropov et al. [89] developed an externally validated one-variable model for C_{60} solubility using additive optimal descriptors calculated from the International Chemical Identifier (InChI) code (Eq. 14-9):

$$\log S = -7.98(\pm 0.14) + 0.325(\pm 0.0010) \, DCW(\text{InChI})$$
$$n = 92, \, R^2 = 0.94, \, Q^2 = 0.94, \, s = 0.25, \, F = 1540, \tag{14-9}$$
$$n_{\text{test}} = 30, \, R^2_{\text{test}} = 0.94, \, s_{\text{test}} = 0.35, \, F_{\text{test}} = 437$$

The descriptor $DCW(\text{InChI})$ is defined as the sum of the correlation weights $CW(I_k)$ for individual IChI attributes I_k characterizing the solvent molecules. The example of the $DCW(\text{InChI})$ calculation is presented in Table 14-2. The values of $CW(I_k)$ were optimized by the Monte Carlo method.

Table 14-2. Illustration of the DCW calculation using pentane as an example (InChI: 1/C5H12/c1-3-5-4-2/h3-5H2,1-2H3). The value of DCW(InChI)=6.9256652 [89]

I_k	$CW(I_k)$
C5	2.0516145
H12	−0.1385480
/	−0.5043203
c1	0.9127424
-3	0.0975796
-5	0.7976968
-4	0.7174808
-2	0.6093029
/	−0.5043203
h3	0.4292022
-5	0.7976968
H2	−0.4992814
-1	0.4421542
-2	0.6093029
H3	1.1073621

All of the above models refer to physico-chemical properties as the endpoints, thus they are also termed quantitative structure–property relationships (QSPRs). Currently, there are only a small number of QSARs related directly to nano-materials' activity. In 2007 Tsakovska [128] proposed the application of QSAR methodology to predict protein–nanoparticle interactions. In 2008 Durdagi et al. published two papers [129, 130] presenting QSAR-based design of novel inhibitors of human immunodeficiency virus type 1 aspartic protease (HIV-1 PR). In the first work [130] the authors developed a three-dimensional QSAR model with compar-ative molecular similarity indices analysis (CoMSIA) method for 49 derivatives of fullerene C_{60}. The values of R^2 and Q^2 for the training set (n=43) were 0.99 and 0.74, respectively. The absolute values of residuals in the validation set (n=6) ranged from 0.25 to 0.99 logarithmic units of EC_{50} (μM). The second model [129] were characterized by lower values of the statistics (n=17, R^2=0.99 and Q^2=0.56). However, in that case the predictions for an external set of compounds (n_{test}=3) were possible with an acceptable level of error. In addition, the authors proposed nine novel structures indicating possible inhibitor activity based on the model obtained. They concluded that steric effects play the most important role in the inhibition mechanism as well as electrostatic and H-donor/acceptor proper-ties. However, the last two types of interactions are of lower importance. Similarly, SMILES-based optimal descriptors have been successfully applied for modeling HIV-1 PR fullerene-based inhibitors [131]. The model reported by Toropov et al. [131] was described by the following equation and parameters:

$$
\begin{aligned}
&pEC50 = -31.6 + 0.125 \ DCW \\
&n = 8 \ R^2 = 0.90 \ Q^2 = 0.85 \ s = 0.35 \ F = 58 \ \text{(subtraining set)} \\
&n = 7 \ R^2 = 0.52 \ Rm^2 = 0.13 \ s = 1.27 \ F = 5 \ \text{(calibration set)} \\
&n = 5 \ R^2 = 0.99 \ Rm^2 = 0.96 \ s = 0.18 \ F = 367 \ \text{(test set)}
\end{aligned}
\tag{14-10}
$$

Rasulev et al. [132] developed a QSAR model for the cytotoxicity to the bac-terium *E. coli* of nano-sized metal oxides. They successfully predicted the toxicity of seven compounds (namely, SnO_2, CuO, La_2O_3, Al_2O_3, Bi_2O_3, SiO_2, and V_2O_3) from the model trained on the other seven oxides (ZnO, TiO_2, Fe_2O_3, Y_2O_3, ZrO_2, In_2O_3, and Sb_2O_3). The model employing the SMILES-based descriptor *DCW* is given by Eq. (14-11):

$$
\begin{aligned}
&-pLD50 = 1.32(\pm 0.031) + 0.27(\pm 0.0080) \ DCW \\
&n = 7, \ R^2 = 0.99, \ s = 0.053, \ F = 539; \\
&n_{\text{test}} = 7, \ R^2_{\text{test}} = 0.82, \ s_{\text{test}} = 0.241, \ F = 23
\end{aligned}
\tag{14-11}
$$

The *DCW* descriptor in this case is defined as the following (Eq. 14-12):

$$
DCW = \sum_{i=1}^{N} CW(SA_k)
\tag{14-12}
$$

where the SA_k is a SMILES attribute, i.e., one symbol (e.g., "O," "=," "V") or two symbols (e.g., "Al," "Bi," "Cu") in the SMILES notation. Numbers of double bonds have been used as global SMILES attributes. They are denoted as "=001" and "=002." "=001" is the indicator of one double bond and "=002" is the indicator of two double bonds.

Although we strongly believe in the usefulness and appropriateness of QSAR methodology for nanomaterial studies, the number of available models related to activity and toxicity is still very limited. When analyzing the situation, it seems that the main limitation is insufficient amount of existing experimental data. In many cases, lack of data precludes an appropriate implementation of statistical methods, including necessary external validation of the model. The problem of the paucity of data will be solved only when a strict collaboration between the experimentalists and QSAR modelers is established. The role of the modelers in such studies should not be restricted only to rationalization of the data after completing the experimental part, but also they must be involved in the planning of the experimentation. Since the experiments on nanomaterials are usually expensive, a kind of compromise between the highest possible number of compounds for testing and the lowest number of compounds necessary for developing a reliable QSAR model should be reached. Regarding the limited amount of data and high costs of the experiments, the idea of applying novel read-across techniques enabling preliminary estimation of data (Chapter 7) [82, 133] is very promising. However, no one has yet tried to implement this technique to nanomaterials.

14.5.   SUMMARY

Without doubt, a large and increasing aspect of the near future of chemistry and technology will be related to the development of nanomaterials. On one hand, due to their extraordinary properties, nanomaterials are becoming a chance for medicine and industry. But, on the other hand, the same properties might result in new pathways and mechanisms of toxic action. In effect, the work with nanomaterials is challenging for both "types" of chemists: those who are searching for and synthesizing new chemicals and those who are working on risk assessment and protection of humans from the effects of these chemicals.

When analyzing the current status of nano-QSAR, the four noteworthy suggestions for further work can be made:

1. There is a strong need to supplement the existing set of molecular descriptors by novel "nanodescriptors" that can represent size-dependent properties of nanomaterials.
2. A stronger than usual collaboration between the experimentalists and nano-QSAR modelers seems to be crucial. On one hand, it is necessary to produce data of higher usefulness for QSAR modelers (more compounds, more systematic experimental studies within groups of structural similarity, etc.). On the other hand, a proper characterization of the nanomaterials structure is not possible only at the theoretical (computational) level. In such situation, experiment-based structural descriptors for nano-QSAR might be required.

3. It is possible that the current criteria of the models'quality (the five OECD rules) will have to be re-evaluated and adapted to nanomaterials. This is due to the specific properties of chemicals occurring at the "nano" level (i.e., electronic properties change with changing size) and the very limited number of data (problems with the "classic" method of validation which is biased to small, low molecular weight molecules).

4. Greater effort is required in the areas of grouping nanomaterials and nano-read-across. This technique might be useful especially at the initial stage of nano-QSAR studies, when the experimental data are scarce.

In summary, the development of reliable nano-QSAR is a serious challenge that offers an exciting new direction for QSAR modelers. This task will have to be completed before the massive production of nanomaterials in order to prevent potentially hazardous molecules from being released into the environment. In the long term, prevention is always more efficient and cheaper than clean-up.

ACKNOWLEDGEMENT

REFERENCES

1. Feynman RP (1959) There's plenty of room at the bottom. An invitation to enter a new field of physics. The Annual Meeting of the American Physical Society, California Institute of Technology (Caltech). http://www.zyvex.com/nanotech/feynman.html. Accessed 6 January 2009

2. Borm PJ, Robbins D, Haubold S et al. (2006) The potential risks of nanomaterials: A review carried out for ECETOC. Part Fibre Toxicol 3:11

3. Serpone N, Dondi D, Albini A (2007) Inorganic and organic UV filters: Their role and efficiency in sunscreens and suncare products. Inorg Chim Acta 360:794–802

4. Cai R, Van GM, Aw PK et al. (2006) Solar-driven self-cleaning coating for a painted surface. CR Chimie 9:829–835

5. Yuranova T, Laub D, Kiwi J (2007) Synthesis activity and characterization of textiles showing self-cleaning activity under daylight irradiation. Catal Today 122:109–117

6. Zhou K, Wang R, Xu B et al. (2006) Synthesis, characterization and catalytic properties of CuO nanocrystals with various shapes. Nanonechnology 17:3939–3943

7. Consumer Products Inventory of Nanotechnology Products (2009) The Project on Emerging Nanotechnologies. http://www.nanotechproject.org/inventories/consumer/. Accessed 15 January 2009

8. Alivisatos P (2004) The use of nanocrystals in biological detection. Nat Biotechnol 22:47–52

9. Chen FQ, Gerion D (2004) Fluorescent CdSe/ZnS nanocrystal-peptide conjugates for long-term, nontoxic imaging and nuclear targeting in living cells. Nano Lett 4:1827–1832

10. Kroto HW, Heath JR, O'Brien SC et al. (1985) C60: Buckminsterfullerene. Nature 318:162–163

11. Iijima S (1991) Helical microtubules of graphitic carbon. Nature 354:56–58

12. Ravi P, Dai S, Wang C et al. (2007) Fullerene containing polymers: A review on their synthesis and supramolecular behavior in solution. J Nanosci Nanotechnol 7:1176–1196

13. Agui L, Yanez-Sedeno P, Pingarron JM (2008) Role of carbon nanotubes in electroanalytical chemistry: A review. Anal Chim Acta 622:11–47

14. Mauter MS, Elimelech M (2008) Environmental applications of carbon-based nanomaterials. Environ Sci Technol 42:5843–5859

15. Chatterjee R (2008) The challenge of regulating nanomaterials. Environ Sci Technol 42:339–343

16. Nel A, Xia T, Madler L et al. (2006) Toxic potential of materials at the nanolevel. Science 311:622–627

17. Li M, Li JC (2006) Size effects on the band-gap of semiconductor compounds. Mater Lett 60:2526–2529

18. Wang N, Wang Z, Aust KT et al. (1997) Room temperature creep behavior of nanocrystalline nickel produced by an electrodeposition technique. Mater Sci Eng A237:150–158

19. Wang Y, Chen M, Zhou F et al. (2002) High tensile ductility in a nanostructured metal. Nature 419:912–915

20. Xing HL, Wang CW, Zhang KF et al. (2004) Recent development in the mechanics of superplasticity and its applications. J Mater Process Technol 151:196–202

21. Mamalis AG (2007) Recent advances in nanotechnology. J Mater Process Technol 181:52–58

22. Sun X (2004) Magnetic properties of nanoparticle assemblies. In: Schwarz JA et al. (eds) Dekker encyclopedia of nanoscience and nanotechnology. Taylor & Francis, London

23. Li Z, Wei L, Gao M et al. (2005) One-pot reaction to synthesize biocompatible magnetite nanoparticles. Adv Mater 17:1001–1005

24. Fujishima A, Rao TN, Tryk DA (2000) Titanium dioxide photocatalysis. J Photochem Photobiol C: Photochem Rev 1:1–21

25. Ohji T, Nakahira A, Hirano T et al. (2005) Tensile creep behavior of alumina/silicon carbide nanocomposite. J Am Ceram Soc 77:3259–3262

26. Dreher KL (2004) Health and environmental impact of nanotechnology: Toxicological assessment of manufactured nanoparticles. Toxicol Sci 77:3–5

27. Oberdorster G (1996) Significance of particle parameters in the evaluation of exposure-dose-response relationships of inhaled particles. Inhal Toxicol 8(Suppl):73–89

28. Borm PJ (2002) Particle toxicology: From coal mining to nanotechnology. Inhal Toxicol 14:311–324

29. Donaldson K, Stone V (2003) Current hypotheses on the mechanisms of toxicity of ultrafine particles. Ann Ist Super Sanita 39:405–410

30. Kreyling WG, Semmler M, Moller W (2004) Dosimetry and toxicology of ultrafine particles. J Aerosol Med 17:140–152

31. Oberdorster G, Oberdorster E, Oberdorster J (2005) Nanotoxicology: An emerging discipline evolving from studies of ultrafine particles. Environ Health Perspect 113:823–839

32. Semmler M, Seitz J, Erbe F et al. (2004) Long-term clearance kinetics of inhaled ultrafine insoluble iridium particles from the rat lung, including transient translocation into secondary organs. Inhal Toxicol 16:453–459

33. Oberdorster G, Sharp Z, Atudorei V et al. (2004) Translocation of inhaled ultrafine particles to the brain. Inhal Toxicol 16:437–445

34. Elder A, Gelein R, Silva V et al. (2006) Translocation of inhaled ultrafine manganese oxide particles to the central nervous system. Environ Health Perspect 114:1172–1178

35. Donaldson K, Stone V, Tran CL et al. (2004) Nanotoxicology. Occup Environ Med 61:727–728

36. SCENIHR (2006) Modified opinion on the appropriateness of the risk assessment methodology in accordance with the technical guidance documents for new and existing substances for assessing the risks of nanomaterials. Scientific Committee on Emerging and Newly Identified Health Risks. Accessed 15 April 2009

37. Oberdorster G, Maynard A, Donaldson K et al. (2005) Principles for characterizing the potential human health effects from exposure to nanomaterials: Elements of a screening strategy. Part Fibre Toxicol 2:8

38. Li N, Sioutas C, Cho A et al. (2003) Ultrafine particulate pollutants induce oxidative stress and mitochondrial damage. Environ Health Perspect 111:455–460

39. Xia T, Kovochich M, Brant J et al. (2006) Comparison of the abilities of ambient and manufactured nanoparticles to induce cellular toxicity according to an oxidative stress paradigm. Nano Lett 6:1794–1807

40. Penn A, Murphy G, Barker S et al. (2005) Combustion-derived ultrafine particles transport organic toxicants to target respiratory cells. Environ Health Perspect 113:956–963

41. Tian F, Cui D, Schwarz H et al. (2006) Cytotoxicity of single-wall carbon nanotubes on human fibroblasts. Toxicol In Vitro 20:1202–1212

42. Chen M, von Mikecz A (2005) Formation of nucleoplasmic protein aggregates impairs nuclear function in response to SiO_2 nanoparticles. Exp Cell Res 305:51–62

43. Yokoyama A, Sato Y, Nodasaka Y et al. (2005) Biological behavior of hat-stacked carbon nanofibers in the subcutaneous tissue in rats. Nano Lett 5:157–161

44. Risom L, Moller P, Loft S (2005) Oxidative stress-induced DNA damage by particulate air pollution. Mutat Res 592:119–137

45. Giles GI, Jacob C (2002) Reactive sulfur species: An emerging concept in oxidative stress. Biol Chem 383:375–388

46. Theresa F (2007) The environmental implications of nanomaterials. In: Monteiro-Riviere N, Tran C (ed) Nanonotoxicology: Characterization, dosing and health effects. Informa Healthcare, New York

47. Sies H (1997) Oxidative stress: Oxidants and antioxidants. Exp Physiol 82:291–295

48. Brown DM, Wilson MR, MacNee W et al. (2001) Size-dependent proinflammatory effects of ultrafine polystyrene particles: A role for surface area and oxidative stress in the enhanced activity of ultrafines. Toxicol Appl Pharmacol 175:191–199

49. Shvedova AA, Kisin ER, Mercer R et al. (2005) Unusual inflammatory and fibrogenic pulmonary responses to single-walled carbon nanotubes in mice. Am J Physiol Lung Cell Mol Physiol 289:L698–L708

50. Donaldson K, Stone V, Clouter A et al. (2001) Ultrafine particles. Occup Environ Med 58:211–216, 199

51. Lyon DY, Fortner JD, Sayes CM et al. (2005) Bacterial cell association and antimicrobial activity of a C60 water suspension. Environ Toxicol Chem 24:2757–2762

52. Sayes CM, Fortner JD, Guo W et al. (2004) The differential cytotoxicity of water-soluble fullerenes. Nano Lett 4:1881–1887

53. Magrez A, Kasas S, Salicio V et al. (2006) Cellular toxicity of carbon-based nanomaterials. Nano Lett 6:1121–1125

54. Gordon T, Chen LC, Fine JM et al. (1992) Pulmonary effects of inhaled zinc oxide in human subjects, guinea pigs, rats, and rabbits. Am Ind Hyg Assoc J 53:503–509

55. Rehn B, Seiler F, Rehn S et al. (2003) Investigations on the inflammatory and genotoxic lung effects of two types of titanium dioxide: Untreated and surface treated. Toxicol Appl Pharmacol 189:84–95

56. Chen Y, Chen J, Dong J et al. (2004) Comparing study of the effect of nanosized silicon dioxide and microsized silicon dioxide on fibrogenesis in rats. Toxicol Ind Health 20:21–27

57. Donaldson K, Tran L, Jimenez LA et al. (2005) Combustion-derived nanoparticles: A review of their toxicology following inhalation exposure. Part Fibre Toxicol 2:10

58. Wiseman H, Halliwell B (1996) Damage to DNA by reactive oxygen and nitrogen species: Role in inflammatory disease and progression to cancer. Biochem J 313:17–29

59. Marnett LJ (2000) Oxyradicals and DNA damage. Carcinogenesis 21:361–370

60. Floyd RA (1990) Role of oxygen free radicals in carcinogenesis and brain ischemia. FASEB J 4:2587–2597

61. Wang B, Feng W, Zhu M et al. (2009) Neurotoxicity of low-dose repeatedly intranasal instillation of nano- and submicron-sized ferric oxide particles in mice. J Nanopart Res 11:41–53

62. Swaiman KF (1991) Hallervorden-spatz syndrome and brain iron metabolism. Arch Neurol 48:1285–1293

63. Bosi S, Feruglio L, Da Ros T et al. (2004) Hemolytic effects of water-soluble fullerene derivatives. J Med Chem 47:6711–6715

64. Dobrovolskaia MA, Aggarwal P, Hall JB et al. (2008) Preclinical studies to understand nanoparticle interaction with the immune system and its potential effects on nanoparticle biodistribution. Mol Pharm 5:487–495

65. Zuin S (2007) Effect-oriented physicochemical characterization of nanomaterials. In: Monteiro-Riviere NA, Tran CL (ed) Nanonotoxicology: Characterization, dosing and health effects. Informa Healthcare, New York

66. Oberdorster E (2004) Manufactured nanomaterials (fullerenes, C60) induce oxidative stress in the brain of juvenile largemouth bass. Environ Health Perspect 112:1058–1062

67. Andrievsky G, Derevyanchenko L, Klochkov V (2007) The myth about toxicity of pure fullerenes is irreversibly destroyed. Eighth Biennial Workshop "Fullerenes and Atomic Clusters" IWFAC'2007, St. Petersburg, Russia. http://www.fullwater.com.ua/Veb%20picture/End%20of%20Myth.htm. Accessed 1 April 2009

68. Lovern SB, Klaper R (2006) *Daphnia magna* mortality when exposed to titanium dioxide and fullerene (C60) nanoparticles. Environ Toxicol Chem 25:1132–1137

69. Andrievsky G, Klochkov V, Derevyanchenko L (2005) Is the C60 fullerene molecule toxic?! Fuller Nanotub Carbon Nanostruct 13:363–376

70. Adams LK, Lyon DY, McIntosh A et al. (2006a) Comparative toxicity of nano-scale TiO_2, SiO_2 and ZnO water suspensions. Water Sci Technol 54:327–334

71. Adams LK, Lyon DY, Alvarez PJ (2006b) Comparative eco-toxicity of nanoscale TiO_2, SiO_2, and ZnO water suspensions. Water Res 40:3527–3532

72. Heinlaan M, Ivask A, Blinova I et al. (2008) Toxicity of nanosized and bulk ZnO, CuO and TiO_2 to bacteria *Vibrio fischeri* and crustaceans *Daphnia magna* and *thamnocephalus platyurus*. Chemosphere 71:1308–1316

73. Smith CJ, Shaw BJ, Handy RD (2007) Toxicity of single walled carbon nanotubes to rainbow trout, (*Oncorhynchus mykiss*): Respiratory toxicity, organ pathologies, and other physiological effects. Aquat Toxicol 82:94–109

74. Mouchet F, Landois P, Sarremejean E et al. (2008) Characterisation and in vivo ecotoxicity evaluation of double-wall carbon nanotubes in larvae of the amphibian *Xenopus laevis*. Aquat Toxicol 87:127–137

75. Todeschini R, Consonni V (2000) Handbook of molecular descriptors. Wiley – VCH Verlag, Weinheim

76. Opera TI, Waller CL, Marshall GR (1994) 3D-QSAR of human immunodeficiency virus (i) protease inhibitors. III. Interpretation of COMFA results. Drug Des Discov 12:29–51

77. Ravi M, Hopfinger AJ, Hormann RE et al. (2001) 4D-QSAR analysis of a set of ecdysteroids and a comparison to COMFA modeling. J Chem Inf Comput Sci 41:1587–1604

78. Mekenyan O, Dimitrov S, Schmieder P et al. (2003) In silico modelling of hazard endpoints: Current problems and perspectives. SAR QSAR Environ Res 14:361–371

79. Kuz'min VE, Artemenko AG, Polischuk PG et al. (2005) Hierarchic system of QSAR models (1d-4d) on the base of simplex representation of molecular structure. J Mol Model 11:457–467

80. Toropov AA, Leszczynski J (2007) A new approach to the characterization of nanomaterials: Predicting young's modulus by correlation weighting of nanomaterials codes. Chem Phys Lett 433:125–129

81. Toropov AA, Leszczynska D, Leszczynski J (2007) Predicting water solubility and octanol water partition coefficient for carbon nanotubes based on the chiral vector. Comput Biol Chem 31:127–128

82. Worth A (2007) Computational nanotoxicology – towards a structure-activity based paradigm for investigation of the activity of nanoparticles. Icon Workshop. Towards Predicting Nano-Bio Interactions, Zurich, Switzerland. Available online at: http://ecb.jrc.it/qsar/information-sources/. Accessed on 05-2008

83. OECD (2007) Guidance document on the grouping of chemicals. Organisation of Economic Cooperation and Development. http://www.oecd.org. Accessed 15 May 2008

84. Maynard AD, Aitken R (2007) Assessing exposure to airborne nanomaterials: Current abilities and future requirements. Nanotoxicology 1:26–41

85. Toropov AA, Benfenati E (2007) Smiles as an alternative to the graph in QSAR modelling of bee toxicity. Comput Biol Chem 31:57–60

86. Toropov AA, Benfenati E (2008) Additive smiles-based optimal descriptors in QSAR modelling bee toxicity: Using rare smiles attributes to define the applicability domain. Bioorg Med Chem 16:4801–4809

87. Toropov AA, Benfenati E (2007a) Optimisation of correlation weights of smiles invariants for modelling oral quail toxicity. Eur J Med Chem 42:606–613

88. Toropov AA, Benfenati E (2007b) Smiles in QSPR/QSAR modeling: Results and perspectives. Curr Drug Discov Technol 4:77–116

89. Toropov AA, Toropova AP, Benfenati E et al. (2009) Additive in chi-based optimal descriptors: QSPR modeling of fullerene C60 solubility in organic solvents. J Math Chem. Published on line: doi: 10.1007/s10910-008-9514-0

90. Toropova AP, Toropov AA, Maksudov SK (2006) QSPR modeling mineral crystal lattice energy by optimal descriptors of the graph of atomic orbitals. Chem Phys Lett 428:183–186

91. Gutman I, Toropov AA, Toropova AP (2005) The graph of atomic orbitals and its basic properties. 1. Wiener index. MATCH Commun Math Comput Chem 53:215–224

92. Gutman I, Furtula B, Toropov AA et al. (2005) The graph of atomic orbitals and its basic properties. 2. Zagreb indices. MATCH Commun Math Comput Chem 53:225–230

93. Churchwell CJ, Rintoul MD, Martin S et al. (2004) The signature molecular descriptor. 3. Inverse-quantitative structure-activity relationship of icam-1 inhibitory peptides. J Mol Graphics Modell 22:263–273

94. Faulon JL, Churchwell CJ, Visco DP Jr (2003) The signature molecular descriptor. 2. Enumerating molecules from their extended valence sequences. J Chem Inf Comput Sci 43:721–734

95. Faulon JL, Collins MJ, Carr RD (2004) The signature molecular descriptor. 4. Canonizing molecules using extended valence sequences. J Chem Inf Comput Sci 44:427–436

96. Faulon JL, Visco DP Jr, Pophale RS (2003) The signature molecular descriptor. 1. Using extended valence sequences in QSAR and QSPR studies. J Chem Inf Comput Sci 43:707–720

97. Jensen F (1999) Introduction to computational chemistry. John Wiley & Sons, Chichester

98. Lee CW, Yang W, Parr RG (1988) Development of the colle-salvetti correlation energy formula into a functional of the electron density. Phys Rev B 37:785–789

99. Becke AD (1993) Density-functional thermochemistry. III The role of exact exchange. J Chem Phys 98:5648–5652

100. Makov G, Payne MC (1995) Periodic boundary conditions in ab initio calculations. Phys Rev B 51:4014–4022

101. Marana NL, Longo VM, Longo E et al. (2008) Electronic and structural properties of the (1010) and (1120) ZnO surfaces. J Phys Chem A 112:8958–8963

102. Beltran A, Andres J, Sambrano JR et al. (2008) Density functional theory study on the structural and electronic properties of low index rutile surfaces for $TiO_2/SnO_2/TiO_2$ and $SnO_2/TiO_2/SnO_2$ composite systems. J Phys Chem A 112:8943–8952

103. Jena P, Castleman AW (2006) Clusters: A bridge across the disciplines of physics and chemistry. Proc Natl Acad Sci USA 103:10560–10569

104. Puzyn T, Michalkova A, Gorb L et al. (2007) A new concept of molecular nanodescriptors for QSAR/QSPR studies. Seventh Southern School on Computational Chemistry and Material Science, Jackson, MS, USA. http://ccmsi.us/sscc_archive/ Accessed 21 August 2009

105. Hassellov M, Readman JW, Ranville JF et al. (2008) Nanoparticle analysis and characterization methodologies in environmental risk assessment of engineered nanoparticles. Ecotoxicology 17:344–361

106. Shukla MK, Leszczynski J (2006) A density functional theory study on the effect of shape and size on the ionization potential and electron affinity of different carbon nanostructures. Chem Phys Lett 428:317–320

107. Yumura T, Nozaki D, Hirahara K et al. (2006) Quantum-size effects in capped and uncapped carbon nanotubes. Annu Rep Prog Chem Sect C: Phys Chem 102:71–79

108. Yumura T, Nozaki D, Bandow S et al. (2005) End-cap effects on vibrational structures of finite-length carbon nanotubes. J Am Chem Soc 127:11769–11776

109. Wang JL, Mezey PG (2006) The electronic structures and properties of open-ended and capped carbon nanoneedles. J Chem Inf Model 46:801–807

110. Poater A, Gallegos Saliner A, Worth A (2007) Modelling nanoneedles: A journey towards nanomedicine. Second Nanotoxicology Conference, Venice, Italy. Available online at: http://ecb.jrc.it/qsar/information-sources/. Accessed 15 May 2008

111. Poater A, Saliner AG, Carbo-Dorca R et al. (2009) Modeling the structure-property relationships of nanoneedles: A journey toward nanomedicine. J Comput Chem 30:275–284

112. Simeon TM, Yanov I, Leszczynski J (2005) Ab initio quantum chemical studies of fullerene molecules with substituents $C_{59}X$ X=Si, Ge, Sn., $C_{59}X^-$ X=B, Al, Ga, In., and $C_{59}X^+$N, P, As, Sb. Int J Quantum Chem 105:429–436

113. Kukreja LM, Barik S, Misra P (2004) Variable band gap ZnO nanostructures grown by pulsed laser deposition. J Cryst Growth 268:531–535

114. Qu ZW, Kroes GJ (2006) Theoretical study of the electronic structure and stability of titanium dioxide clusters $(TiO_2)_n$ with n=1-9. J Phys Chem B 110:8998–9007

115. Zhai HJ, Wang LS (2007) Probing the electronic structure and band gap evolution of titanium oxide clusters $(TiO_2)_n^-$ (n=1−10) using photoelectron spectroscopy. J Am Chem Soc 129:3022–3026

116. Limbach LK, Li Y, Grass RN et al. (2005) Oxide nanoparticle uptake in human lung fibroblasts: Effects of particle size, agglomeration, and diffusion at low concentrations. Environ Sci Technol 39:9370–9376

117. Brunner TJ, Wick P, Manser P et al. (2006) In vitro cytotoxicity of oxide nanoparticles: Comparison to asbestos, silica, and the effect of particle solubility. Environ Sci Technol 40:4374–4381

118. Mackay D, Shiu WY, Ma K-C et al. (2007) Handbook of physical-chemical properties and environmental fate for organic chemicals. Taylor & Francis, Boca Raton, London, New York

119. Toxnet toxicology data network (2009) United States National Library of Medicine. http://toxnet.nlm.nih.gov/. Accessed 1 April 2009

120. Ormsby JL, King BT (2004) Clar valence bond representation of pi-bonding in carbon nanotubes. J Org Chem 69:4287–4291

121. Martin D, Maran U, Sild S et al. (2007) QSPR modeling of solubility of polyaromatic hydrocarbons and fullerene in 1-octanol and n-heptane. J Phys Chem B 111:9853–9857

122. Marcus Y, Smith AL, Korobov MV et al. (2001) Solubility of fullerene. J Phys Chem B 105:2499–2506

123. Murray JS, Gagarin SG, Politzer P (1995) Representation of C_{60} solubilities in terms of computed molecular surface electrostatic potentials and areas. J Phys Chem 99:12081–12083

124. Sivaraman N, Srinivasan TG, Vasudeva Rao PR et al. (2001) QSPR modeling for solubility of fullerene (C_{60}) in organic solvents. J Chem Inf Comput Sci 41:1067–1074

125. Kiss IZ, Mandi G, Beck MT (2000) Artificial neural network approach to predict the solubility of C60 in various solvents. J Phys Chem A 104:8081–8088

126. Liu H, Yao X, Zhang R et al. (2005) Accurate quantitative structure–property relationship model to predict the solubility of C60 in various solvents based on a novel approach using a least-squares support vector machine. J Phys Chem B 109:10565–20571

127. Katritzky AR, Karelson M, Petrukhin R (2001–2005) CODESSA PRO. Comprehensive descriptors for structural and statistical analysis. http://www.codessa-pro.com. Accessed 15 October 2008

128. Tsakovska I, Gallegos Saliner A, Bassan A et al. (2007) Computational modelling of nanoparticles. Second Nanotoxicology Conference, Venice, Italy. Available online at: http://ecb.jrc.it/qsar/information-sources/. Accessed 05-2008

129. Durdagi S, Mavroumoustakos T, Papadopoulos MG (2008) 3D QSAR COMFA/COMSIA, molecular docking and molecular dynamics studies of fullerene-based HIV-1 pr inhibitors. Bioorg Med Chem Lett 18:6283–6289

130. Durdagi S, Mavroumoustakos T, Chronakis N et al. (2008) Computational design of novel fullerene analogues as potential HIV-1 pr inhibitors: Analysis of the binding interactions between fullerene inhibitors and HIV-1 pr residues using 3D QSAR, molecular docking and molecular dynamics simulations. Bioorg Med Chem 16:9957–9974

131. Toropov AA, Toropova AP, Benfenati E et al. (2009) SMILES-based optimal descriptors: QSAR analysis of fullerene-based HIV-1 PR inhibitors by means of balance of correlations. J Comput Chem (accepted)

132. Rasulev BF, Toropov AA, Puzyn T et al. (2007) An application of Graphs of Atomic Orbitals for QSAR modeling of toxicity of metal oxides. 34th Annual Federation of Analytical Chemistry and Spectroscopy Societies, Memphis, TN, USA

133. Saliner AG, Poater A, Worth AP (2008) Toward in silico approaches for investigating the activity of nanoparticles in therapeutic development. IDrugs 11:728–732